Check for updates

Received: 18 October 2019 | Revised: 19 February 2020 | Accepted: 9 March 2020

DOI: 10.1111/ejn.14724

SPECIAL ISSUE ARTICLE

EJN European Journal of Neuroscience FENS WILEY

IP_3R2 null mice display a normal acquisition of somatic and neurological development milestones

Sónia Guerra-Gomes[1,2] | Daniela Cunha-Garcia[1,2] | Diana Sofia Marques Nascimento[1,2] | Sara Duarte-Silva[1,2] | Eduardo Loureiro-Campos[1,2] | Vanessa Morais Sardinha[1,2] | João Filipe Viana[1,2] | Nuno Sousa[1,2] | Patrícia Maciel[1,2] | Luísa Pinto[1,2] | João Filipe Oliveira[1,2,3]

[1]Life and Health Sciences Research Institute (ICVS), School of Medicine, University of Minho, Braga, Portugal

[2]ICVS/3B's – PT Government Associate Laboratory, Braga/Guimarães, Portugal

[3]Applied Artificial Intelligence Laboratory, IPCA-EST-2Ai, Polytechnic Institute of Cávado and Ave, Barcelos, Portugal

Correspondence
João Filipe Oliveira, Life and Health Sciences Research Institute (ICVS), School of Medicine, University of Minho, Campus de Gualtar, 4710-057 Braga, Portugal.
Email: joaooliveira@med.uminho.pt

Funding information
Foundation for Science and Technology (FCT), Grant/Award Number: IF/01079/2014, IF/00328/2015, PTDC/MED-NEU/31417/2017, POCI-01-0145-FEDER-016818 and POCI-01-0145-FEDER-007038; Bial Foundation, Grant/Award Number: 207/14, 037/18 and 427/14; European Regional Development Fund (FEDER), Grant/Award Number: NORTE-01-0145-FEDER-000013

Abstract

Astrocytes are key players in the regulation of brain development and function. They sense and respond to the surrounding activity by elevating their intracellular calcium (Ca^{2+}) levels. These astrocytic Ca^{2+} elevations emerge from different sources and display complex spatio-temporal properties. Ca^{2+} elevations are spatially distributed in global (soma and main processes) and/or focal regions (microdomains). The inositol 1,4,5-trisphosphate receptor type 2 knockout (IP_3R2 KO) mouse model lacks global Ca^{2+} elevations in astrocytes, and it has been used by different laboratories. However, the constitutive deletion of IP_3R2 during development may trigger compensating phenotypes, which could bias the results of experiments using developing or adult mice. To address this issue, we performed a detailed neurodevelopmental evaluation of male and female IP_3R2 KO mice, during the first 21 days of life, as well as an evaluation of motor function, strength and neurological reflexes in adult mice. Our results show that male and female IP_3R2 KO mice display a normal acquisition of developmental milestones, as compared with wild-type (WT) mice. We also show that IP_3R2 KO mice display normal motor coordination, strength and neurological reflexes in adulthood. To exclude a potential compensatory overexpression of other IP_3Rs, we quantified the relative mRNA levels of all 3 subtypes, in brain tissue. We found that, along with the complete deletion of *Itpr2*, there is no compensatory expression of *Itpr1* or *Itrp3*. Overall, our results show that the IP_3R2 KO mouse is a reliable model to study the functional impact of global IP_3R2-dependent astrocytic Ca^{2+} elevations.

KEYWORDS

astrocytes, behaviour, calcium signalling, development, IP_3R2

Abbreviations: ANOVA, analysis of variance; Ca^{2+}, calcium ion; IP_3, inositol 1,4,5-trisphosphate; IP_3R2 KO, inositol 1,4,5-trisphosphate receptor type 2 knockout; IP_3R2, inositol 1,4,5-trisphosphate receptor type 2; PCR, polymerase chain reaction; PND, postnatal day; SEM, standard error of the mean; SHIRPA, SmithKline Beecham Pharmaceuticals; Harwell, MRC Mouse Genome Centre and Mammalian Genetics Unit; Imperial College School of Medicine at St Mary's; Royal London Hospital, St Bartholomew's and the Royal London School of Medicine; Phenotype Assessment; WT, wild-type.

Edited by Ania Majewska.

The peer review history for this article is available at https://publons.com/publon/10.1111/ejn.14724

© 2020 Federation of European Neuroscience Societies and John Wiley & Sons Ltd

1 | INTRODUCTION

Astrocytes, the most abundant glial cell type in the nervous system, play a pivotal role in integrating and responding to network activity (Mederos, González-Arias, & Perea, 2018; Oliveira, Sardinha, Guerra-Gomes, Araque, & Sousa, 2015; Perea, Navarrete, & Araque, 2009). Phylogenetic evidence showing an increased glia-to-neuron ratio, namely in species with larger brains (Verkhratsky & Nedergaard, 2016), support the importance of this role of astrocytes. These glial cells sense and integrate the surrounding activity by elevating its intracellular calcium (Ca^{2+}) levels. The discovery of this particular astrocytic feature and the development of tools to allow its quantification (Cornell-Bell, Finkbeiner, Cooper, & Smith, 1990; Nedergaard, 1994; Parpura et al., 1994) paved the way for a better understanding of the spatio-temporal dynamics of astrocytic modulation (Shigetomi, Patel, & Khakh, 2016; Volterra, Liaudet, & Savtchouk, 2014). Since then, several studies described important contributions of astrocytic Ca^{2+} signalling for the control of synaptic communication, circuit computation and behavioural performance (Guerra-Gomes, Sousa, Pinto, & Oliveira, 2018). Astrocyte activation can elicit complex Ca^{2+} events that vary from global (mainly observed in the soma and main processes) to focal (restricted to thin processes and microdomains), whose complexity and functional consequences are being studied by multiple laboratories (Shigetomi et al., 2016; Volterra et al., 2014). Taking advantage of the high predominance of inositol 1,4,5-trisphosphate receptor type 2 (IP_3R2) in astrocytes, the most used animal model to study the role of global IP_3-dependent Ca^{2+} elevations in astrocytes is the knockout mouse for this receptor (IP_3R2 KO; Li, Zima, Sheikh, Blatter, & Chen, 2005). This model displays an intact neuronal Ca^{2+} activity, but critically impaired global astrocytic Ca^{2+} signals, and therefore, it has been extensively used both in health and disease contexts (Agulhon, Fiacco, & McCarthy, 2010; Cao et al., 2013; Guerra-Gomes, Viana, et al., 2018; Jego, Pacheco-Torres, Araque, & Canals, 2014; Li et al., 2015; Navarrete et al., 2012; Okubo et al., 2019; Petravicz, Fiacco, & McCarthy, 2008; Pinto-Duarte, Roberts, Ouyang, & Sejnowski, 2019; Rakers & Petzold, 2017; Sherwood et al., 2017; Srinivasan et al., 2015; Takata et al., 2011; Tanaka, Wang, Mikoshiba, Hirase, & Shinohara, 2017; Wang, Xu, Wang, Takano, & Nedergaard, 2012; Yang et al., 2016).

These mice are viable and fertile and display no major alterations in brain cytoarchitecture (Li et al., 2005; Petravicz et al., 2008). However, the constitutive nature of the IP_3R2 deletion might lead to alterations that could influence experimental results obtained during development and adult stages. To address this issue, we performed a detailed examination of somatic parameters and neurological reflexes acquired during development, in male and female IP_3R2 KO mice and respective wild-type (WT) littermates. Moreover, we complemented this analysis by assessing general phenotypical behaviour in adult mice through the analysis of motor behaviour and exploratory drive. Our results show that IP_3R2 KO mice display a normal acquisition of somatic and neurodevelopmental milestones, as well as unaffected locomotor or exploratory abilities in adulthood. Therefore, they are suitable for functional testing during development and adult stages.

2 | MATERIALS AND METHODS

2.1 | Animals

All experimental procedures were conducted in accordance with the guidelines described in Directive 2010/63/EU and were approved by the local ethical committee (SECVS 075/2015), and the national authority for animal experimentation (DGAV 17469/2012). A mouse strain with targeted deletion of *Itpr2* gene was kindly supplied for this project by Prof. Alfonso Araque (U. Minnesota, USA; Navarrete et al., 2012), under agreement with Prof. Ju Chen (U.C. San Diego, USA; Li et al., 2005). Mice were backcrossed at least 5 generations to C57BL/6J. All mice had ad libitum access to food and water in their home cages, and lights were maintained on a 12-hr light/dark cycle (lights on 8:00 a.m. to 8:00 p.m.) at 22 ± 1°C, 55% humidity, as described in previous studies (Kafetzopoulos et al., 2018; Mateus-Pinheiro et al., 2017; Sardinha et al., 2017; Tavares et al., 2017). IP_3R2 KO and their respective littermate WT controls were obtained by mating couples of $IP_3R2^{+/-}$. A total of 19 WT (9 males and 10 females) and 20 littermate IP_3R2 KO mice (10 males and 10 females) were used to perform a neurodevelopmental evaluation. All animals received a toe tag at postnatal day (PND) 5 as described in Castelhano-Carlos, Sousa, Ohl, and Baumans (2010), which remained unaltered throughout the experiment and allowed to evaluate each animal response in a blind manner. The collected toe tissue was used for DNA extraction and subsequent genotyping by polymerase chain reaction (PCR) analysis using WT (F, 5′-ACCCTGATGAGGGAAGGTCT-3′; R, 5′-ATCGATTCATAGGGCACACC-3′) and mutant allele-specific primers (neo-specific primer: F, 5′-AATG GGCTGACCGCTTCCTCGT-3′; R, 5′-TCTGAGAGTGC CTGGCTTTT-3′) as previously described (Li et al., 2005). For adult motor function assessment, we used male and female groups of WT and littermate IP_3R2 KO mice (n = 6–12 per group) of 3 to 4 month old. Tissue from these WT and IP_3R2 KO mice (n = 3 per group) was used for the *Itpr* gene expression assessment.

14609568, 2021, 5, Downloaded from https://onlinelibrary.wiley.com/doi/10.1111/ejn.14724 by Universidade Do Minho, Wiley Online Library on [16/10/2026]. See the Terms and Conditions (https://onlinelibrary.wiley.com/terms-and-conditions) on Wiley Online Library for rules of use; OA articles are governed by the applicable Creative Commons License

2.2 | Behaviour analyses: developmental milestones

Neonatal neurodevelopmental milestones were assessed according to previously validated protocols in mice (Castelhano-Carlos et al., 2010; Hill, Lim, & Stone, 2008; Santos, Silva-Fernandes, Oliveira, Sousa, & Maciel, 2007). It consisted of a daily evaluation for 21 days, since the day of birth. At birth, only the number of pups in the litter was counted without any further examination. From PND1 onwards, newborn animals were inspected for skin appearance, activity and presence of a milk spot in the stomach, which are indicators for correct maternal care and well-being. Moreover, animals were daily weighted and examined for the acquisition of developmental milestones until weaning (PND21). This daily scoring included the assessment of the acquisition of a mature response regarding several somatic and neurological parameters. Pups were tested every day at the same time, in the same experimental room, by the same experimenters. Throughout the evaluation, several parameters were assessed according to the age of the pup (Figure 1a), and the score value was registered in an individual table for each animal.

2.2.1 | Somatic parameters

Body weight was registered every day from PND1 to PND21 (weight ± 0.01 g), as an indicator of morphological development. Anogenital distance, which corresponds to the distance between the opening of the anus and the opening of the genitalia, is a marker for reproductive development and maturation. This parameter was daily registered starting from PND3

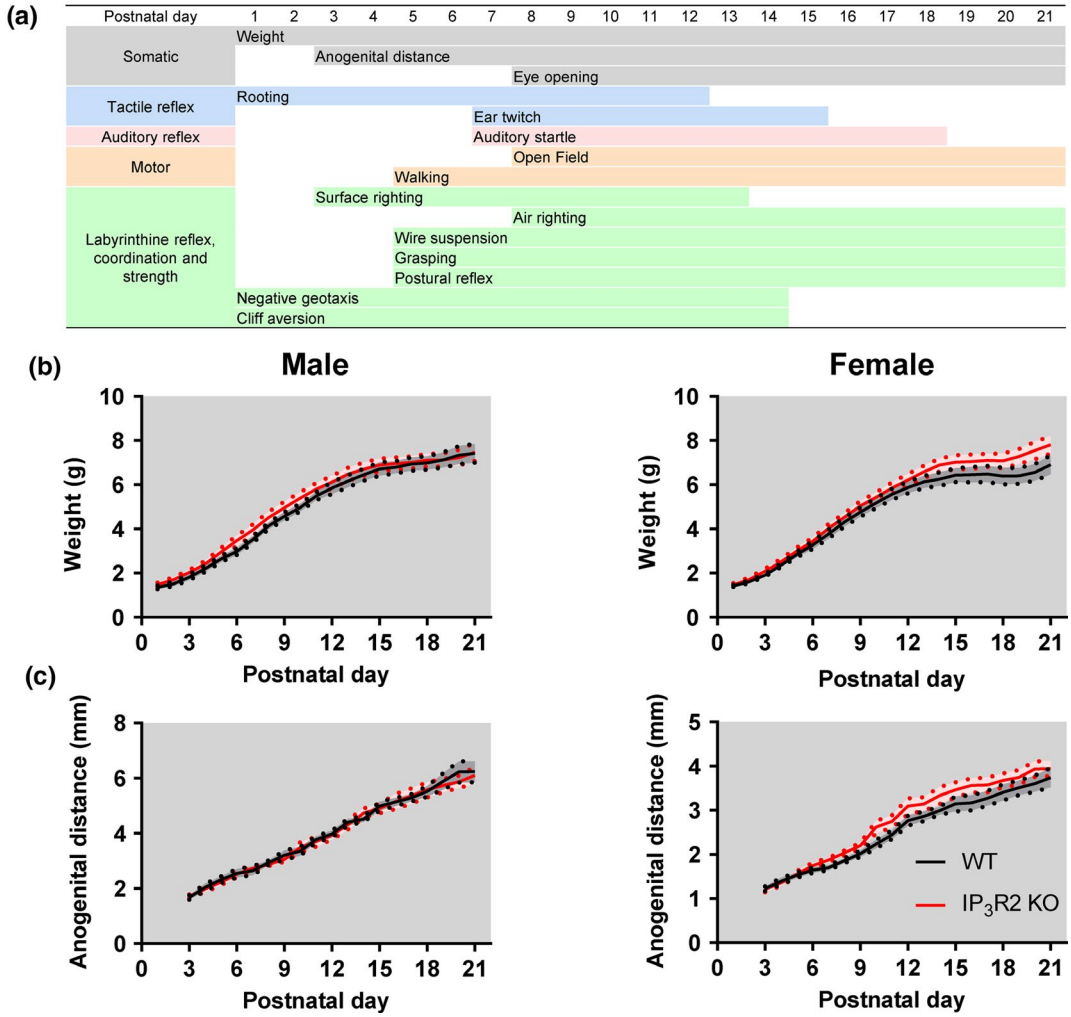


FIGURE 1 Male and female IP_3R2 KO mice gain weight similarly to controls and display a normal genital development. (a) Representative scheme of the experimental timeline used, depicting each developmental parameter according to the tested function (grey—somatic parameters, blue—tactile reflex, pink—auditory reflex, orange—motor function, green—labyrinthine reflex, coordination and strength). (b) Body weight evolution from postnatal day 1 to postnatal day 21 of WT and IP_3R2 KO mice. (c) Anogenital distance evolution from postnatal day 3 to postnatal day 21 of WT and IP_3R2 KO mice. Males are represented in left panels, and female mice are depicted in right panels (WT—black, IP_3R2 KO—red). Data plotted as mean ± *SEM*. $n = 9–10$ per group

14609568, 2021, 5, Downloaded from https://onlinelibrary.wiley.com/doi/10.1111/ejn.14724 by Universidade Do Minho, Wiley Online Library on [16/10/2026]. See the Terms and Conditions (https://onlinelibrary.wiley.com/terms-and-conditions) on Wiley Online Library for rules of use; OA articles are governed by the applicable Creative Commons License

(distance ± 0.05 mm). Eye opening was daily scored according to the state of the eyes. Eye opening was considered when an initial break in the membrane sealing was observed. When one of the eyes was opened, a score of 1 was attributed; when both eyes were opened, a score of 2 was achieved. PND of mature response was registered when both eyes were open.

2.2.2 | Neurological reflexes

Neurological reflexes were daily assessed from PND1 to PND21. Cages containing the mother and pups were taken from the housing room to an experimental room at the same circadian rhythm hour. To ensure the minimal disturbance of the pups, tests were performed on a smooth foam pad, and after the evaluation, pups were immediately returned to the home cage. The daily score was attributed as following: tests that evaluated absence/presence of a mature response were scored as 0/1 (rooting, ear twitch, auditory startle, open field traversal, air righting, wire suspension, postural reflex); parameters where a gradual evolution was observable were scored from 0 to 3 (walking, surface righting, grasping, negative geotaxis, cliff aversion), with 0 representing absence and 3 corresponding to achievement of the mature response. In the end, PND of mature response achievement was registered for each pup. Neurological reflexes were divided into several categories according to the function analysed, and they were assessed as follows:

Tactile reflex

Rooting—This test consists in gently stroking a fine filament of cotton three times along the side of the head of the pup. If it turns the head towards the filament, a mature response is considered.

Ear twitch—It consisted in stimulating the ear of the pup by brushing it with the end of a cotton tip three times. If the newborn responded by flattening the ear against the side of the head, a score for a mature response was attributed.

Auditory reflex

Auditory startle—Newborn mice were tested for auditory reflex from PND7 until PND18. The response of the animal to a handclap was observed. If the animal reacted, then a mature response was achieved and a score of 1 was attributed.

Motor

Open field traversal—Newborn mice (PND8-21) were placed in the centre of a plastic sheet containing a circle with 13 cm of diameter. The time that the animal took to move out of the circle was recorded. A mature response was considered when the mouse was able to respond in <30 s. This test allows the evaluation of locomotion and the extinction of pivoting behaviour.

Walking—The development of locomotion and coordination was evaluated by observing animals freely moving, from PND5 until PND21. The mature response was considered when pups were able to walk straight with their body completely supported by the four limbs.

Labyrinthine reflex, coordination and strength

Surface righting reflex—This parameter was evaluated from PND1 until PND13. It consisted in putting the animal on its back, and the mature response was considered when the animal was able to get right. It evaluates spatial, body righting and labyrinthine mechanisms.

Air righting reflex—This parameter was assessed from PND8 until PND21. Mice were turned back and held at approximately 13 cm distance from the soft surface and released. A mature response was observed when the pup developed the reflex to turn his body during the fall and land on its four paws.

Postural reflex—Mice response was assessed from PND5 until weaning. Animals were placed in a small plastic open box and gently shaken vertically and horizontally. If the animal maintained its original position in the box, it was assumed to have acquired a mature postural reflex response. This parameter allows the evaluation of spatial and body righting responses.

Negative geotaxis—This behavioural response was evaluated from PND1 until PND14. Pups were placed in a horizontal grid, tilted 45° to the plane, with its head facing downwards. It was considered a mature response when the animal was able to turn immediately by 180° and moved towards the top of the slope. It tests spatial, body righting and labyrinthine mechanisms.

Cliff aversion—It evaluates the ability of mice to turn and crawl away when put on the edge of a cliff, with its forepaws and face over the edge (from PND1 until PND14). This parameter allows the assessment of spatial reflex and coordination.

Wire suspension—This parameter evaluates forelimb grasp and was assessed from PND5 until the weaning age. This strength test consists in placing the pup vertically to hold a 2-mm metal bar with its forelimbs. A mature response was achieved when the animal was able to hold its body weight alone, without falling.

Grasping—This is a strength test performed from PND5 until PND21. The forelimb of the pup was stimulated with a thin wire. If the animal held the wire firmly, a mature response was considered.

2.3 | Behaviour analyses: adult phenotyping

Adult behaviour was analysed according to previously validated protocols in mice (Carter et al., 1999;

14609568, 2021, 5, Downloaded from https://onlinelibrary.wiley.com/doi/10.1111/ejn.14724 by Universidade Do Minho, Wiley Online Library on [16/10/2026]. See the Terms and Conditions (https://onlinelibrary.wiley.com/terms-and-conditions) on Wiley Online Library for rules of use; OA articles are governed by the applicable Creative Commons License

Silva-Fernandes et al., 2014; Teixeira-Castro et al., 2015). Behaviour tests were performed during the diurnal period. Motor coordination was assessed using the open field test, the beam walk balance test, motor swimming test and the footprint analysis. Furthermore, strength and neurological reflexes were assessed through the hanging wire grid test and additional tests from the SHIRPA protocol (Rogers et al., 2001).

2.3.1 | Motor function

Open field

The open field test was used to assess spontaneous locomotor and exploratory activity (Seibenhener & Wooten, 2015). The apparatus consisted of a brightly illuminated Plexiglas box enclosing a white arena (43.2 × 43.2 × 30.5 cm), equipped with infrared beams to detect mice activity (Med Associates Inc). Mice were individually placed in the centre of the arena and let to freely explore it for 5 min. This test allowed the assessment of motor (by the distance walked) and exploratory activity (by the number of vertical rearings).

Motor swimming tests

These tests were used to evaluate voluntary locomotion, by taking advantage of survival instinct of mice to escape from the water and find a safe shelter. Swimming tests were conducted in two tanks with water at 23 ± 1°C, under dim light conditions. The water was made opaque using non-toxic titanium dioxide (Sigma-Aldrich, 250 mg/L) to improve mice detection (Sardinha et al., 2017). The distance and time swam were monitored and analysed by a video-tracking system (Viewpoint). The first test was conducted in a dark circular pool with 106 cm diameter. Each mouse was gently placed in the pool and allowed to swim freely during 60 s, and the total distance swam during this period was registered. In the second test, each mouse was placed at one end of rectangular tank (100 cm long and 15 cm depth) and trained during 2 consecutive days (3 trials/day), to reach a visible platform at the opposite end (60 cm). In the following 3 days (2 trials/day), mice were tested, and the time taken to cross the water tank was registered.

Beam walk balance test

Balance and fine motor coordination were evaluated by the latency of each mouse to traverse elevated narrow beams to a safe platform. Beams consisted of long strips of PVC (1 m) with a 12 mm square cross-section or 11 mm round diameter. Beams were placed horizontally, 50 cm above the bench surface (covered with soft sponges to protect mice from falls), with one end mounted on a narrow support and the other end attached to an enclosed dark box (20 cm square), into which mice could escape. Mice were trained during 3 consecutive days in the square beam (3 trials/animal), and in the fourth day, the animals were tested in both beams (2 trials/animal). The time taken to cross the beams was recorded.

Footprint analysis

Mice hind and forepaws were coated with black and red non-toxic ink, respectively, and encouraged to walk an inclined corridor (100 cm × 4.2 cm width × 10 cm height; over white absorbent paper) towards a black box. Footprint patterns obtained for each mouse were used to analyse gait. Three measurements were registered, for six consecutive steps, to evaluate mice stride length.

2.3.2 | Strength and neurological reflexes

Behaviour tests followed the SHIRPA Protocol guidelines, enriched with the hanging wire grid test (Silva-Fernandes et al., 2014; Teixeira-Castro et al., 2015).

Wire maneuver—Mice were picked by the tail, and forelimbs were placed to a fixed wire (soft sponges were placed underneath to protect falling mice). This test is based on the latency of a mouse to fall off a metal wire upon exhaustion. The maximum duration of the test was 120 s.

Hanging wire grid test—Mice were placed on the top of a metallic horizontal grid and inverted 180º towards the surface of the bench (soft sponges were placed underneath to protect falling mice). This test measures the latency to fall off a metal grid upon exhaustion. The maximum duration of the test was 120 s.

Strength to grab—Mice were placed in the metal grid and then were gently pulled backwards by the tail in a horizontal plane. The instinct of mice was to grab the grid, which allowed to score the force applied by the mouse as 0—normal (active) or 1—abnormal (light to moderate).

Limb grasping—The animal is picked up by the tail and slowly inclined towards a horizontal surface. Close to the surface, mice clasped or not front and/or hind feet. This neurological reflex behaviour was scored as 0—absent or 1—present.

Limb clasping—The animal was picked by the tail and gently descended towards a horizontal surface. During the descending movement, the mice extend all four limbs in anticipation of contact and we evaluated the limb clasping as 0—absent, 1—present in one paw (mild) or 2—two paws (severe).

2.4 | Molecular analysis: macrodissection, RNA isolation, cDNA synthesis and real-time quantitative (RT-q)PCR analysis

In order to assess the transcription levels of the three distinct IP_3Rs isoforms (IP_3R1, IP_3R2, IP_3R3), relative mRNA levels of these genes were quantified by RT-qPCR. Animals were first anaesthetized with a mixture of ketamine (75 mg/

14609568, 2021, 5, Downloaded from https://onlinelibrary.wiley.com/doi/10.1111/ejn.14724 by Universidade Do Minho, Wiley Online Library on [16/10/2026]. See the Terms and Conditions (https://onlinelibrary.wiley.com/terms-and-conditions) on Wiley Online Library for rules of use; OA articles are governed by the applicable Creative Commons License

kg, i.p.; Imalgene 1000, Merial, EUA) and medetomidine (1 mg/kg, i.p.; Dorbene Vet, Pfizer, EUA) and transcardially perfused with 0.9% saline. Brains were harvested and immediately flash frozen in liquid nitrogen and carefully removed. Hippocampi were rapidly macrodissected and stored at −80°C until further analysis.

Total hippocampal RNA (WT and IP_3R2 KO, $n = 3$ per group) was isolated using QIAzol lysis reagent (Qiagen). Briefly, tissue was mechanically homogenized in QIAzol reagent with a syringe and 20G needle. Following addition of chloroform and centrifugation, the RNA-containing upper phase was retrieved. Isopropanol was used for RNA precipitation, and formed pellets were washed in ethanol 75%. After air-drying, RNA pellets were resuspended in RNAse-free water and concentration of isolated RNA measured in a Nanodrop 2000. Total RNA (500 ng) was then reverse-transcribed using qScript™ cDNA SuperMix (Quanta Biosciences). The following primers were designed using PRIMER-BLAST (NCBI, http://www.ncbi.nlm.nih.gov/tools/primer-blast/) and used for expression quantification: *Hprt* (F 5′-GCTGGTGAAAAGGACCTCT-3′; R 5′-CAGAGGACTAGAACACCTGC-3′); *Itpr1* (F 5′-CTCT GTATGCGGAGGGATCTAC-3′; R 5′-GCGGAGTATCGATT CATAGGAC-3′); *Itpr2* (F 5′-CTTCCTCTACATTGG GGACATC-3′; R 5′-GGCAGAGTATCGATTCATAGGG-3′); *Itpr3* (F 5′-AGCCAAGCAGACTAAACAGGAC-3′; R 5′-GCCGCTTGTTCACAGTTAAGTA-3′). Quantification was performed using the Fast Real-Time PCR System (Applied Biosystems) and 5× HOT FIREPol® EvaGreen® qPCR Mix Plus, ROX (Solis Biodyne). Target gene expression levels were normalized against the housekeeping gene *Hprt*, and the relative expression was calculated using the ΔCt method. Fold changes to the WT group were also calculated and plotted for the three genes.

2.5 | Statistical analysis

Developmental milestones were performed and analysed by the same researchers, who were blind to the mouse genotype during the protocol. Prism 7 (GraphPad Software Inc.) was used to assess normal distributions and further group comparisons. Continuous variables followed a Gaussian distribution (Kolmogorov–Smirnov test) within groups, and parametric tests were applied, while non-parametric tests were used for discrete variables. Two-way analysis of variance (ANOVA) with Sidak post hoc test was applied to analyse somatic parameters, considering either factors: postnatal day and genotype. Multiple *t* tests were applied for open field, swimming in the circular pool, footprint and wire maneuver in adult mice. Mann–Whitney test was used to analyse the remaining tests and RT-qPCR data. For the comparison of categorical variables (strength to grab, limb grasping and clasping), crosstabulations were performed and the statistical test used was Fisher's exact test (when Pearson chi-squared assumptions were not met). Data are expressed either as mean ± *SEM* (Standard Error of the Mean), as median, or as percentage as stated in the legend. The results were considered statistically significant for a $p < .05$.

3 | RESULTS

WT and IP_3R2 KO newborn mice included in this study received correct maternal care and welfare. They were daily evaluated for the acquisition of several somatic and neurological responses, during the first 21 days of life (Figure 1a).

3.1 | IP_3R2 KO mice display a normal somatic development

Somatic parameters assessed during the developmental milestones protocol in WT and IP_3R2 KO mice were body weight, anogenital distance and eye opening (Figure 1a, grey).

Results show that male WT and IP_3R2 KO mice display a body weight increase along time (Figure 1b; $F_{20,340} = 329.0$, $p < .001$), which was similar between genotypes ($F_{1,17} = 0.62$, $p = .44$). Female mice daily increased their body weight (Figure 1b; $F_{20,360} = 278.4$, $p < .001$), and this parameter was also similar between WT and IP_3R2 KO littermates ($F_{1,18} = 2.001$, $p = .170$).

The anogenital distance in male WT and IP_3R2 KO mice equivalently increased along time (Figure 1c; $F_{18,288} = 197.1$, $p < .001$), and no differences were observed between genotypes ($F_{1,16} = 0.04$, $p = .84$). Similarly, WT and IP_3R2 KO female mice displayed a daily increase in anogenital distance (Figure 1c; $F_{18,324} = 185.5$, $p < .001$), which was not significantly different between genotypes ($F_{1,18} = 2.54$, $p = .13$). Regarding eye opening, WT and IP_3R2 KO mice from both sexes acquired the mature response simultaneously (male: $U = 38.0$; $p = .60$; female: $U = 40.5$; $p = .46$; Figure 2a). Altogether, these results are indicators that the constitutive genetic deletion of IP_3R2 does not interfere with general growth during the development of male and female newborn mice.

3.2 | IP_3R2 KO mice display an intact acquisition of neurodevelopmental milestones

Neurodevelopmental evaluation included the examination of several neurological parameters related to sensorial (Figure 1a, blue and pink) and motor functions (Figure 1a, orange), labyrinthine reflex, coordination and strength (Figure 1a, green) in male and female WT and IP_3R2 KO mice. Tactile reflex development was evaluated in rooting and ear twitch tests (Figure 2b). Our results show that male WT and IP_3R2 KO mice display a similar mature response in the rooting test

14609568, 2021, 5, Downloaded from https://onlinelibrary.wiley.com/doi/10.1111/ejn.14724 by Universidade Do Minho, Wiley Online Library on [16/10/2026]. See the Terms and Conditions (https://onlinelibrary.wiley.com/terms-and-conditions) on Wiley Online Library for rules of use; OA articles are governed by the applicable Creative Commons License

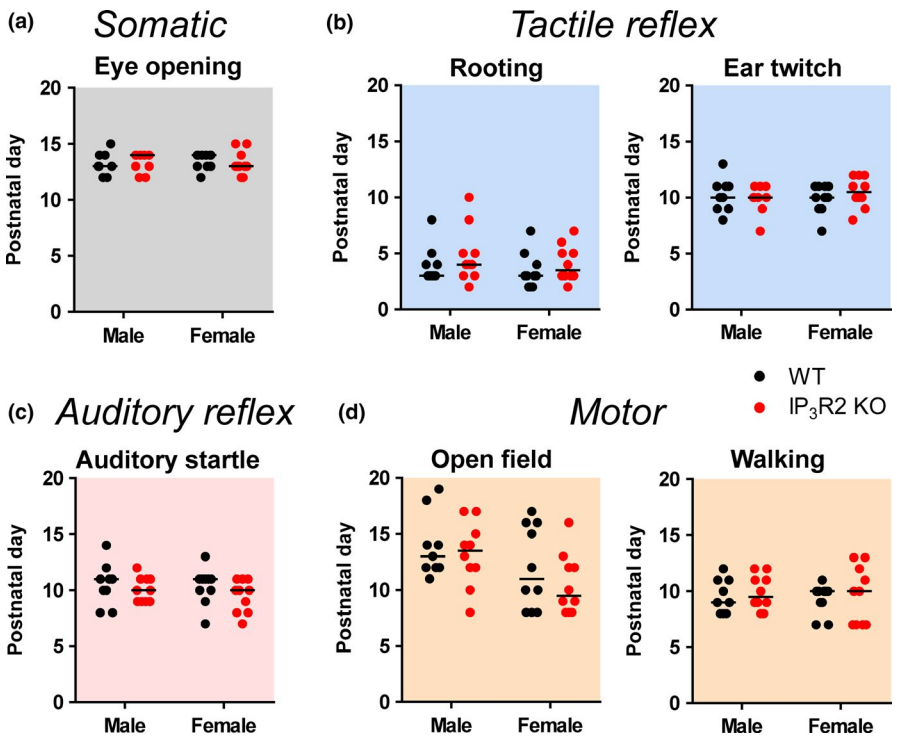


FIGURE 2 Male and female IP_3R2 KO mice retain a normal acquisition of somatic and sensory-motor parameters. (a) Day of acquisition of a somatic milestone (eye opening, grey background). (b–d) Day of acquisition of neurological reflexes related to sensorial (b, c) and motor function (d). (b) Rooting and ear twitch tests were performed to evaluate the developmental acquisition of tactile reflex (blue background). (c) Day of acquisition of a mature auditory reflex (pink background). (d) Open field and walking are parameters for the assessment of a mature locomotor response (orange background). WT mice are represented in black, and IP_3R2 KO mice are represented in red (males, left column; females, right column). Dots represent individuals; dash represents the median. $n = 9–10$ per group

($U = 34.5$; $p = .40$), which was equivalently observed for females ($U = 35.5$; $p = .29$). More so, ear twitch test revealed no significant differences between WT and IP_3R2 KO mice from both sexes (male: $U = 41.5$; $p = .78$; female: $U = 37.5$; $p = .36$). Auditory system development was assessed by the auditory startle test. We observed that male WT and IP_3R2 KO newborn mice equally acquired this milestone (Figure 2c; $U = 38.0$; $p = .58$), and females from both genotypes displayed a similar mature response ($U = 32.5$; $p = .19$). The achievement of motor abilities is a good indicator of neurological development. We evaluated motor function in the open field traversal and walking tests (Figure 2d). Our results show an equal acquisition of the mature response in the open field traversal for male ($U = 42.5$; $p = .86$) and female ($U = 39.5$; $p = .44$) mice from both genotypes. Furthermore, male WT and IP_3R2 KO mice equally acquired a mature walking ability ($U = 38.5$; $p = .63$), which was also observed for females from both genotypes ($U = 43.5$; $p = .63$).

The neurological milestone evaluation also comprises tests to evaluate the vestibular system formation, namely surface righting, air righting, postural reflex, negative geotaxis and cliff aversion (Figure 3). In the surface righting test, we evaluated labyrinthine reflex and coordination. We found no differences between male WT and IP_3R2 KO mice in this test ($U = 40.5$; $p = .73$). A similar mature response was also observed for female WT and IP_3R2 KO mice ($U = 33.5$; $p = .21$). In the air righting test, male WT and IP_3R2 KO displayed an analogous mature response ($U = 34.0$; $p = .38$), which was also observed for females ($U = 49.5$; $p = .97$). Moreover, we found that genetic deletion of IP_3R2 did not alter postural reflex acquisition in males ($U = 37.5$; $p = .56$) and females ($U = 38.5$; $p = .38$). In the negative geotaxis test, the mature response of male IP_3R2 KO mice was reached similarly to WT littermates ($U = 42.0$; $p = .83$). Female WT and IP_3R2 KO mice also equally acquired this developmental milestone ($U = 43.0$; $p = .59$). Lastly, cliff aversion test showed that male WT and IP_3R2 KO mice present a mature response approximately at the same postnatal day ($U = 42.0$; $p = .82$), which was also confirmed for female IP_3R2 KO mice ($U = 31.0$; $p = .16$). Another important measure of postnatal development is strength. We assessed this parameter by performing wire suspension and grasping test (Figure 3). Our results show that male WT and IP_3R2 KO mice display a similar mature response in wire suspension ($U = 44.5$; $p = .98$), which was again confirmed for IP_3R2 KO female mice ($U = 26.0$; $p = .06$). Overall, this detailed assessment of neurological parameters shows that IP_3R2 KO mice acquire all mature responses for sensory-motor functions, vestibular area-dependent tasks, and strength similarly to WT.

14609568, 2021, 5, Downloaded from https://onlinelibrary.wiley.com/doi/10.1111/ejn.14724 by Universidade Do Minho, Wiley Online Library on [16/10/2026]. See the Terms and Conditions (https://onlinelibrary.wiley.com/terms-and-conditions) on Wiley Online Library for rules of use; OA articles are governed by the applicable Creative Commons License

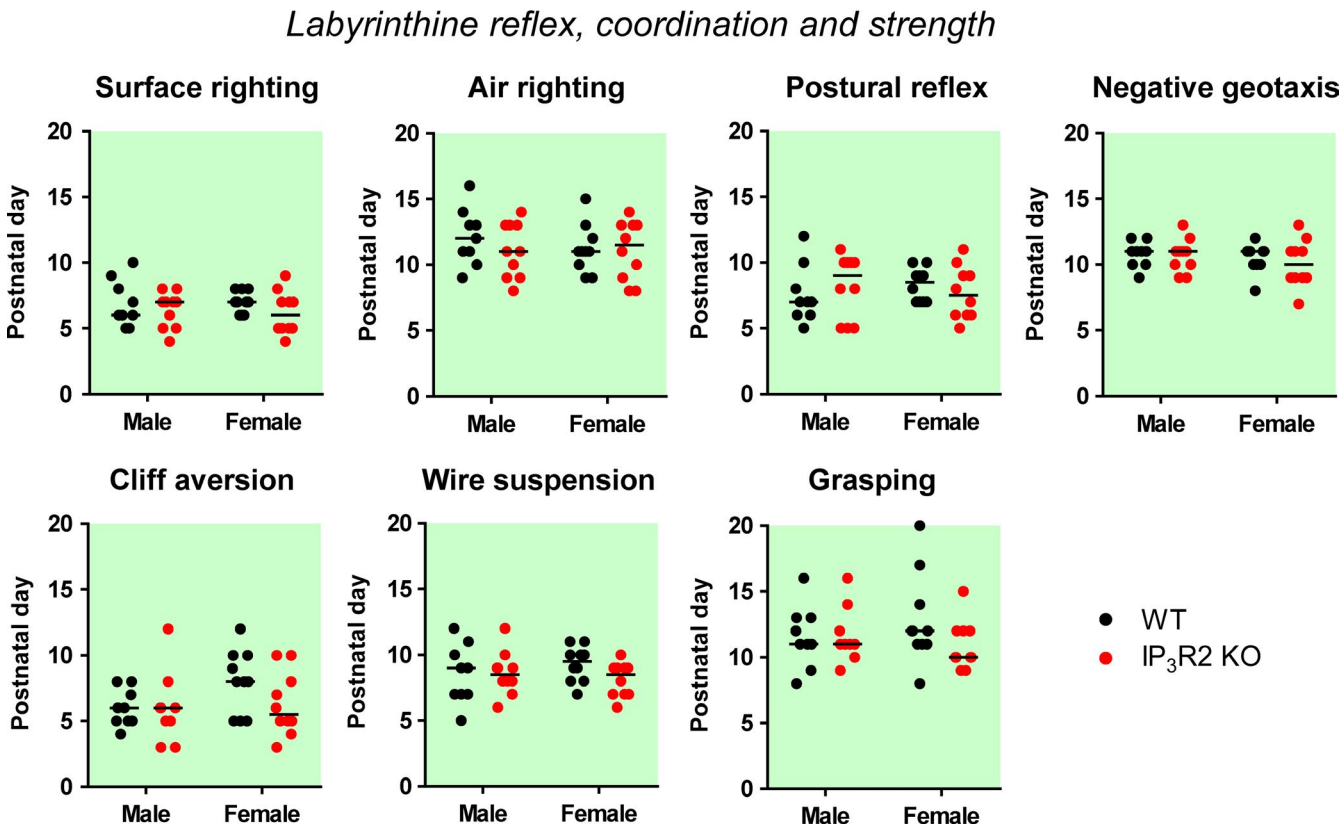


FIGURE 3 Male and female IP_3R2 KO mice display normal labyrinthine reflex, coordination and strength. Day of acquisition of the mature response of surface righting, air righting, postural reflex, negative geotaxis, cliff aversion, wire suspension and grasping as measures of vestibular system formation and strength acquisition. WT mice are represented in black, and IP_3R2 KO mice are represented in red (males, left column; females, right column). Dots represent individuals; dash represents the median. $n = 9–10$ per group

3.3 | IP_3R2 KO adult mice display normal motor function and exploratory behaviour

The analysis of developmental milestone acquisition showed that the constitutive deletion of IP_3R2 does not interfere with the normal acquisition of somatic and neurological parameters. Nevertheless, we also aimed to assess locomotor and exploratory function in adult WT and IP_3R2 KO mice, both in males and females. The open field test provided us with measures of ambulatory behaviour and motor function, such as distance travelled and number of vertical rearings (Figure 4a). Male and female IP_3R2 KO mice travelled similar distances as controls (males: $t_{11} = 0.91$; $p = .38$; females: $t_{11} = 2.02$; $p = .07$). Regarding exploratory behaviour, no differences between male WT and IP_3R2 KO mice were observed for the number of rearings ($t_{11} = 0.63$; $p = .54$). Female IP_3R2 KO display a similar number of vertical rearings when compared to WT mice ($t_{11} = 1.32$; $p = .21$). Next, we analysed the distance swam by each mouse during 60 s in the circular pool (Figure 4b). Results showed that IP_3R2 KO mice travelled similar distances, as compared with control littermates, for both males ($t_{14} = 1.44$; $p = .17$) and females ($t_{14} = 1.35$; $p = .20$). Furthermore, we analysed the time animals took to traverse a water tank (fixed distance of 60 cm; Figure 4b). We found no differences between WT and IP_3R2 KO both in males ($U = 41.0$; $p = .22$) and females ($U = 27.5$; $p = .61$). Next, we performed the beam walk balance test using either a square beam, or a round beam (increased difficulty; Figure 4c). In both cases, IP_3R2 KO animals performed similarly to WT (square, males: $U = 51.5$; $p = .87$; females: $U = 15.0$; $p = .08$; round, males: $U = 48.0$; $p = .70$; females: $U = 27.0$; $p = .59$). To assess the gait of IP_3R2 KO mice, we analysed footprint patterns (Figure 4d) and we observed similar stride lengths among genotypes and sexes (males: $t_{20} = 0.51$; $p = .61$; females: $t_{15} = 1.36$; $p = .20$). To deepen our knowledge on the phenotype of IP_3R2 KO in adulthood, we further assessed muscular strength and neurological reflexes (Figure 5a,b, respectively). We found that WT and IP_3R2 KO mice of both sexes display similar forelimb strength evaluated by the wire maneuver test (males: $t_{19} = 0.75$; $p = .47$; females: $t_{15} = 0.32$; $p = .75$). Additionally, the four-limb muscular strength was also found equivalent in the hanging wire grid test both in male ($U = 54.0$; $p = .69$) and in female ($U = 27.0$; $p = .51$) IP_3R2 KO when compared to their WT-littermate controls. To complement the muscular strength tests, we further assessed qualitatively their strength to grab a grid. Once again,

14609568, 2021, 5, Downloaded from https://onlinelibrary.wiley.com/doi/10.1111/ejn.14724 by Universidade Do Minho, Wiley Online Library on [16/10/2026]. See the Terms and Conditions (https://onlinelibrary.wiley.com/terms-and-conditions) on Wiley Online Library for rules of use; OA articles are governed by the applicable Creative Commons License

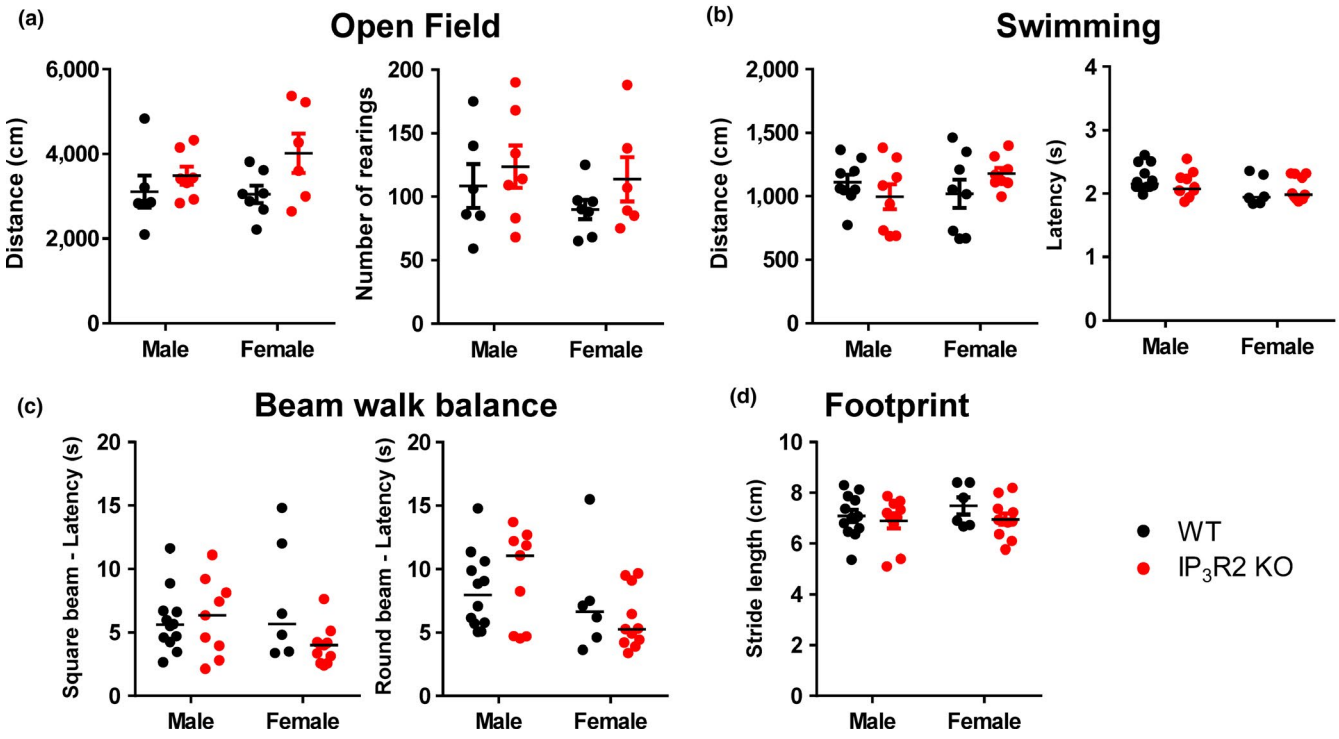


FIGURE 4 Adult IP_3R2 KO mice display normal motor coordination. (a) Distance travelled and number of rearings recorded in the open field test. (b) Distance freely swam in the circular pool during 60 s (left); latency to reach the platform located at 60 cm (right). (c) Latency to cross the square or round beams. (d) Stride length in a 100 cm runway. WT mice are represented in black, and IP_3R2 KO mice are represented in red (males, left column; females, right column). Dots represent individuals; mean ± *SEM* or median. n = 6–12 per group

WT and IP_3R2 KO mice scored similarly (males: p = .714, *Fisher's exact test*; females: *constant variable;* Figure 5a). Absence of limb grasping and limb clasping is a normal neurological reflex in mice. Our tests confirmed that IP_3R2 KO animals (Figure 5b) behave normally also in these tests (grasping males or females: *constant variable*; clasping in males: p = .774 and females: p = .676, *Fisher's exact test*). Altogether, these results confirm that the normal acquisition of the neurodevelopmental milestones observed above is consistent with normal motor coordination, strength and neurological reflexes in adulthood.

3.4 | IP_3R2 KO mice express normal levels of *Itpr1* and *Itrp3*

Assessment of gene expression of the three IP_3Rs isoforms by RT-qPCR demonstrates that both IP_3R1 and IP_3R2 (*Itpr1* and *Itpr2*, respectively) are abundantly expressed in the hippocampus of WT adult mice, while IP_3R3 mRNA levels are expressed in comparatively much lower levels (Figure 6a). Importantly, it is here confirmed that IP_3R2 expression is totally abrogated in adult IP_3R2 KO mice as the levels of *Itpr2* gene expression in these mice drop to values similar to assay blank controls (Figure 6b). In contrast, the expression of the remaining receptors is unaltered between genotypes (Figure 6b; *Itpr1*: U = 2.0; p = .40; *Itpr3*: U = 1.0; p = .20). These findings constitute a relevant validation for the specific and selective knockout of *Itpr2* gene in IP_3R2 KO mice.

4 | DISCUSSION

This comprehensive evaluation of somatic parameters and neurological reflexes shows that the constitutive deletion of IP_3R2 does not interfere with the normal neurodevelopmental milestones acquisition, suggesting a normal development of the nervous system in this mouse model. This is an important observation since this model has been used by multiple laboratories to study the role of astrocytes in health and disease contexts, resulting occasionally in contradictory results (Guerra-Gomes, Sousa, et al., 2018; Oliveira et al., 2015). The IP_3R2 KO model described in 2005 (Li et al., 2005) presents a constitutive gene deletion; that is, the deletion is present throughout embryonic development and may result

14609568, 2021, 5, Downloaded from https://onlinelibrary.wiley.com/doi/10.1111/ejn.14724 by Universidade Do Minho, Wiley Online Library on [16/10/2026]. See the Terms and Conditions (https://onlinelibrary.wiley.com/terms-and-conditions) on Wiley Online Library for rules of use; OA articles are governed by the applicable Creative Commons License

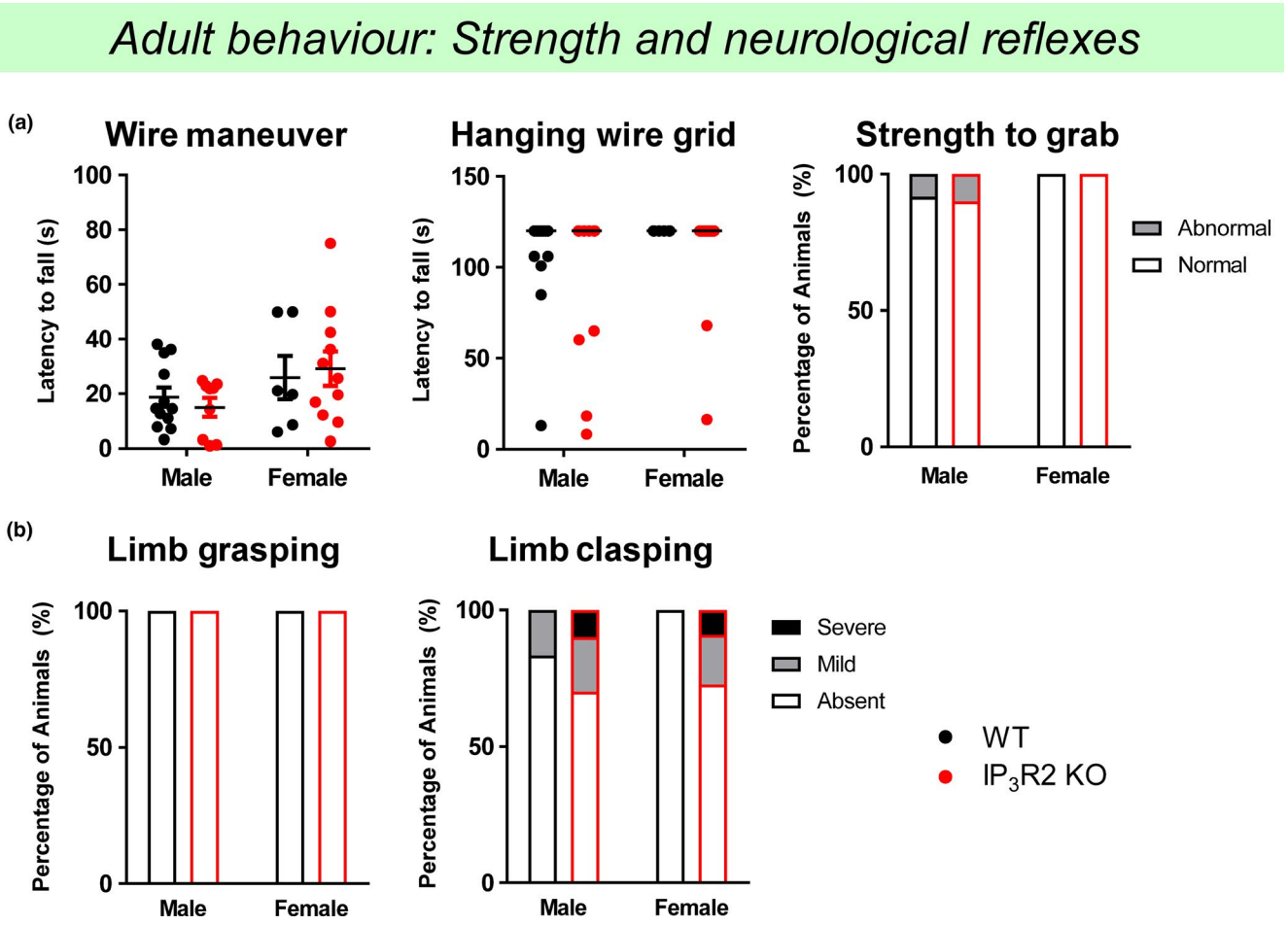


FIGURE 5 Adult IP_3R2 KO mice display normal strength and neurological reflexes. (a) Evaluation of strength by the latency to fall off the wire, and off the metal grid, and the force applied by the mouse to grab the grid. (b) Evaluation of neurological reflexes of limb grasping and clasping upon suspension by the tail; WT mice are represented in black, and IP_3R2 KO mice are represented in red (males, left column; females, right column). Dots represent individuals; mean ± *SEM* or median or percentage of animals for each score. $n = 6–12$ per group

in developmental impairments and/or compensatory mechanisms that could bias experimental results obtained at different ages: development and adulthood. Until now, no studies addressed the influence of IP_3R2 genetic deletion during the postnatal period.

We started by performing a detailed evaluation of neurodevelopmental milestones that consisted of a thorough examination of the somatic parameters and neurological reflexes. Our results showed that IP_3R2 KO mice displayed a body weight increase similar to controls, both in males and females. This result is in line with previous studies showing that adult WT and IP_3R2 KO mice display a similar body weight (Li et al., 2015; Pinto-Duarte et al., 2019). More so, anogenital distance is not altered in both IP_3R2 KO males and females, indicating a normal sexual differentiation in this mouse model. This result is in accordance with the normal colony breeding observed in our laboratory and with a previous report indicating that this mouse strain displays normal reproductive behaviour (Petravicz et al., 2008). Regarding eye opening, our results are in line with the typical age described for the acquisition of this developmental milestone, which is on average at PND13 (Heyser, 2004). These evidences indicate that IP_3R2 KO mice display a healthy physical maturation.

A neurodevelopmental assessment is fundamental to determine and discard possible alterations that might influence brain function and behaviour performance (Sousa, Almeida, & Wotjak, 2006). We examined the acquisition of several neurological parameters related to sensory-motor reflexes, locomotion, coordination and strength in both WT and IP_3R2 KO mice (males and females). In our study, we found that WT and IP_3R2 KO mice similarly acquired a mature response for sensory-motor and auditory reflexes. These responses are in accordance with the average age previously described for C57BL/6 mice (Heyser, 2004; Kleiber, Wright, & Singh, 2011). From these evidences, we expect IP_3R2 KO mice to be able to perform behavioural tests that depend on the tactile, auditory and motor abilities. Another battery of developmental tests covered a progressive maturation of sensory and motor skills depending on the vestibular system maturation (Khan et al., 2004). In these tests, such as surface righting, air righting, postural

14609568, 2021, 5, Downloaded from https://onlinelibrary.wiley.com/doi/10.1111/ejn.14724 by Universidade Do Minho, Wiley Online Library on [16/10/2026]. See the Terms and Conditions (https://onlinelibrary.wiley.com/terms-and-conditions) on Wiley Online Library for rules of use; OA articles are governed by the applicable Creative Commons License

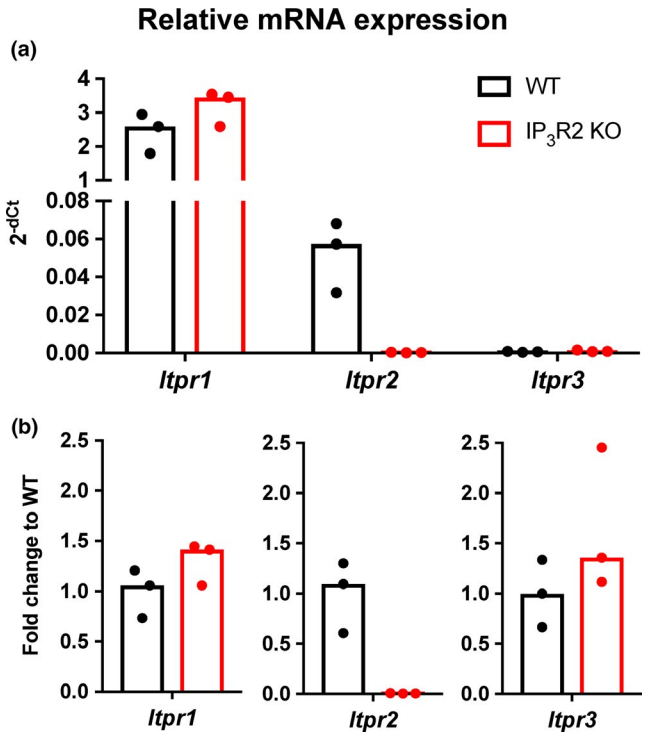


FIGURE 6 The deletion of IP_3R2 does not interfere with the levels of IP_3R1 or IP_3R3. (a) Relative expression levels of IP_3Rs in the hippocampus of WT and IP_3R2 KO mice measured by RT-qPCR. (b) Expression levels relatively to the respective WT levels. WT mice are represented in black, and IP_3R2 KO mice are represented in red. Bar size represents the median. $n = 3$ per group

reflex, negative geotaxis and cliff aversion, no significant differences were detected between WT and IP_3R2 KO mice from both sexes. This reflects a normal acquisition of sensorimotor-related parameters by IP_3R2 KO mice, which discards the existence of possible compensatory mechanisms occurring in vestibular system-related functions during postnatal development. In accordance, in the wire suspension and grasping tests, we found that WT and IP_3R2 KO mice equally performed this test within the typical range for the appearance of these developmental milestones (Heyser, 2004; Kleiber et al., 2011). These tests are related to the acquisition of balance control mechanisms, which are intimately dependent on visual afferent information (Mesquita et al., 2007). It is noteworthy that by backcrossing the original mouse (Li et al., 2005) to C57BL/6J, we eliminated the retinal degeneration and associated loss of visual capacity described to mice that carry Black Swiss background. Overall, these data provide evidence for a normal somatic and neurological development of IP_3R2 KO mice, and they represent the first attempt to assess the influence of the constitutive genetic deletion of IP_3R2.

We further assessed the general motor and exploratory phenotype of adult WT and IP_3R2 KO mice. In the open field test, we analysed two motor-related measures: distance travelled and rearings. The first parameter corresponds to a pure measure of motor ability, while the second one is more related with exploratory drive (Seibenhener & Wooten, 2015). Next, we performed a battery of behavioural tests to obtain readouts of motor coordination, strength and neurological reflexes in adulthood (Rogers et al., 2001; Silva-Fernandes et al., 2014; Teixeira-Castro et al., 2015). In all these tests, the performance of IP_3R2 KO mice was indistinguishable from their littermate WT mice, regardless of the mouse gender. This extensive analysis suggests that IP_3R2 KO mice display a regular motor function and exploratory behaviour in adulthood, which is in line with a normal development of nervous system structures relevant for motor function. These observations are also in accordance with other studies (Cao et al., 2013; Kim et al., 2016; Petravicz, Boyt, & McCarthy, 2014; Pinto-Duarte et al., 2019; Tanaka et al., 2013). Regarding their cognitive, emotional or sensory phenotypes the available studies are still unclear. For instance, IP_3R2 KO mice do not display an anxious phenotype (Cao et al., 2013; Petravicz et al., 2014; Pinto-Duarte et al., 2019; Tanaka et al., 2013), but in what concerns depressive-like behaviour results are contradictory. IP_3R2 KO mice generated on a Black Swiss background display increased learned helplessness (Cao et al., 2013), in opposition to an IP_3Rs knocking-down approach, which leads to an antidepressant phenotype (Galeotti, Vivoli, Norcini, Bartolini, & Ghelardini, 2008). Finally, the specific deletion of IP_3R2 in astrocytes affects neither depressive-like behaviour nor impulsivity (Petravicz et al., 2014). The use of mouse models with consistent genetic background and cellular specificity might help to clarify conflicting results (Oliveira et al., 2015; Yu, Nagai, & Khakh, 2020).

Apart from the direct influence of IP_3R2 deletion, one should consider the possible modulation of behaviour either by compensatory expression of IP_3Rs or changes in interaction between IP_3R2 and other targets. Regarding the first, we confirmed that the hippocampal mRNA levels of IP_3R2 decrease to undetectable levels in IP_3R2 KO mice, while the expression of the other two isoforms (IP_3R1 and IP_3R3) remains unchanged. These results support the specific deletion of the IP_3R2 in our animal model without the compensatory expression of other IP_3Rs, which is in line with (a) the initial study showing selective elimination of IP_3R2 protein in atrial extracts of IP_3R2 KO mice (Li et al., 2005), and (b) with the lack of global calcium signals selectively in astrocytes demonstrated by different laboratories (Navarrete et al., 2012; Petravicz et al., 2008). Regarding the latter, in this work we studied specifically the impact of the constitutive deletion of IP_3R2 to the acquisition of neurological reflexes and motor function. However, we should not rule out possible implications of the IP_3R2 function to other forms of behaviour either during development or in adulthood. For instance, there is an intimate interaction between IP_3R2 and mGluR5 (whose levels change dramatically during the first weeks of life), namely those regulated by Homer1 scaffolding proteins (Buscemi

14609568, 2021, 5, Downloaded from https://onlinelibrary.wiley.com/doi/10.1111/ejn.14724 by Universidade Do Minho, Wiley Online Library on [16/10/2026]. See the Terms and Conditions (https://onlinelibrary.wiley.com/terms-and-conditions) on Wiley Online Library for rules of use; OA articles are governed by the applicable Creative Commons License

et al., 2017) that might have implications in autism spectrum disorders (Petrelli & Bezzi, 2018). The impact of IP_3R2 KO deletion to such complex forms of behaviour needs to be carefully addressed.

Deletion of IP_3R2 in mice emerged as a promising genetic tool to study astrocytic Ca^{2+} signalling (Navarrete et al., 2012; Petravicz et al., 2008; Takata et al., 2011). Advances in the analysis of astrocytic Ca^{2+} elevations showed that astrocytes display rather complex spatial and temporal properties, whose functional consequences are still far from fully understood (Shigetomi et al., 2016; Volterra et al., 2014). Therefore, the field clearly needs tools to tackle differentially global or focal Ca^{2+} elevations. Functionally, the IP_3R2 KO mouse model is an excellent tool to study the roles of global Ca^{2+} elevations specifically in astrocytes as shown by different laboratories (Di Castro et al., 2011; Guerra-Gomes, Viana, et al., 2018; Mederos et al., 2019; Navarrete et al., 2012; Yu et al., 2018). Recently, by employing a viral tool to genetically drive the continuous extrusion of cytosolic Ca^{2+} in astrocytes, Yu et al. (2018) yielded similar levels of impairment of global events, which confirms the functional relevance of the IP_3R2 KO mice. This observation, together with our present findings, fully supports the use of the IP_3R2 KO mouse for the study of astrocyte involvement in all developmental stages and adulthood.

ACKNOWLEDGEMENTS

The authors are grateful to Prof. Alfonso Araque and Prof. Ju Chen for sharing the mice line. They acknowledge also funding from national funds through Foundation for Science and Technology (FCT) fellowships to SGG, ELC, VMS, CEEC to DSMN; IF grants to LP (IF/01079/2014) and JFO (IF/00328/2015); projects PTDC/MED-NEU/31417/2017 and POCI-01-0145-FEDER-016818; Bial Foundation Grants 207/14 and 037/18 to JO, and 427/14 to LP; Northern Portugal Regional Operational Programme (NORTE 2020), under the Portugal 2020 Partnership Agreement, through the European Regional Development Fund (FEDER) (NORTE-01-0145-FEDER-000013); FEDER Funds, through the Competitiveness Factors Operational Programme (COMPETE); and The National Fund, through the FCT (POCI-01-0145-FEDER-007038).

CONFLICT OF INTEREST

The authors declare no conflicts of interest.

AUTHOR CONTRIBUTIONS

SGG, DCG, SDS and DSMN designed and performed the experiments, analysed the data and wrote the manuscript; ELC participated in experimental conception and design; VMS and JFV participated in experimental conception and data analysis; and NS, PM, LP and JFO supervised the study, secured funding, analysed the data and wrote the manuscript.

DATA AVAILABILITY STATEMENT

The data that support the findings of this study are available by request to the corresponding author Dr. João Filipe Oliveira.

ORCID

Sónia Guerra-Gomes https://orcid.org/0000-0002-6717-8941
Daniela Cunha-Garcia https://orcid.org/0000-0001-6090-3517
Diana Sofia Marques Nascimento https://orcid.org/0000-0003-3765-4801
Sara Duarte-Silva https://orcid.org/0000-0001-9680-4027
Eduardo Loureiro-Campos https://orcid.org/0000-0001-5834-5851
João Filipe Viana https://orcid.org/0000-0002-6851-0520
Nuno Sousa https://orcid.org/0000-0002-8755-5126
Patrícia Maciel https://orcid.org/0000-0002-0920-6350
Luísa Pinto https://orcid.org/0000-0002-7724-0446
João Filipe Oliveira https://orcid.org/0000-0002-1005-2328

REFERENCES

Agulhon, C., Fiacco, T. A., & McCarthy, K. D. (2010). Hippocampal short- and long-term plasticity are not modulated by astrocyte Ca^{2+} signaling. *Science*, *327*, 1250–1254.

Buscemi, L., Ginet, V., Lopatar, J., Montana, V., Pucci, L., Spagnuolo, P., … Bezzi, P. (2017). Homer1 scaffold proteins govern Ca^{2+} dynamics in normal and reactive astrocytes. *Cerebral Cortex*, *27*, 2365–2384.

Cao, X., Li, L.-P., Wang, Q., Wu, Q., Hu, H.-H., Zhang, M., … Gao, T.-M. (2013). Astrocyte-derived ATP modulates depressive-like behaviors. *Nature Medicine*, *19*, 773–777.

Carter, R. J., Lione, L. A., Humby, T., Mangiarini, L., Mahal, A., Bates, G. P., … Morton, A. J. (1999). Characterization of progressive motor deficits in mice transgenic for the human Huntington's disease mutation. *Journal of Neuroscience*, *19*, 3248–3257.

Castelhano-Carlos, M. J., Sousa, N., Ohl, F., & Baumans, V. (2010). Identification methods in newborn C57BL/6 mice: A developmental and behavioural evaluation. *Laboratory Animals*, *44*, 88–103.

Cornell-Bell, A. H., Finkbeiner, S. M., Cooper, M. S., & Smith, S. J. (1990). Glutamate induces calcium waves in cultured astrocytes: long-range glial signaling. *Science*, *247*, 470–473.

Di Castro, M. A., Chuquet, J., Liaudet, N., Bhaukaurally, K., Santello, M., Bouvier, D., … Volterra, A. (2011). Local Ca^{2+} detection and modulation of synaptic release by astrocytes. *Nature Neuroscience*, *14*, 1276–1284.

Galeotti, N., Vivoli, E., Norcini, M., Bartolini, A., & Ghelardini, C. (2008). An antidepressant behaviour in mice carrying a gene-specific InsP3R1, InsP3R2 and InsP3R3 protein knockdown. *Neuropharmacology*, *55*, 1156–1164.

14609568, 2021, 5, Downloaded from https://onlinelibrary.wiley.com/doi/10.1111/ejn.14724 by Universidade Do Minho, Wiley Online Library on [16/10/2026]. See the Terms and Conditions (https://onlinelibrary.wiley.com/terms-and-conditions) on Wiley Online Library for rules of use; OA articles are governed by the applicable Creative Commons License

Guerra-Gomes, S., Sousa, N., Pinto, L., & Oliveira, J. F. (2018). Functional roles of astrocyte calcium elevations: From synapses to behavior. *Frontiers in Cellular Neuroscience*, *11*, 427. https://doi.org/10.3389/fncel.2017.00427

Guerra-Gomes, S., Viana, J. F., Nascimento, D. S. M., Correia, J. S., Sardinha, V. M., Caetano, I., … Oliveira, J. F. (2018). The role of astrocytic calcium signaling in the aged prefrontal cortex. *Frontiers in Cellular Neuroscience*, *12*, 379. https://doi.org/10.3389/fncel.2018.00379

Heyser, C. J. (2004). Assessment of developmental milestones in rodents. *Current Protocols in Neuroscience*, Chapter *8*, Unit 8.18.

Hill, J. M., Lim, M. A., & Stone, M. M. (2008). Developmental milestones in the newborn mouse. In I. Gozes (Ed.), *Neuropeptide techniques, neuromethods* (pp. 131–149). Totowa, NJ: Humana Press.

Jego, P., Pacheco-Torres, J., Araque, A., & Canals, S. (2014). Functional MRI in mice lacking IP3-dependent calcium signaling in astrocytes. *Journal of Cerebral Blood Flow and Metabolism*, *34*, 1599–1603.

Kafetzopoulos, V., Kokras, N., Sotiropoulos, I., Oliveira, J. F., Leite-Almeida, H., Vasalou, A., … Dalla, C. (2018). The nucleus reuniens: A key node in the neurocircuitry of stress and depression. *Molecular Psychiatry*, *23*, 579–586.

Khan, Z., Carey, J., Park, H. J., Lehar, M., Lasker, D., & Jinnah, H. A. (2004). Abnormal motor behavior and vestibular dysfunction in the stargazer mouse mutant. *Neuroscience*, *127*, 785–796.

Kim, S. K., Hayashi, H., Ishikawa, T., Shibata, K., Shigetomi, E., Shinozaki, Y., … Nabekura, J. (2016). Cortical astrocytes rewire somatosensory cortical circuits for peripheral neuropathic pain. *Journal of Clinical Investigation*, *126*, 1983–1997.

Kleiber, M. L., Wright, E., & Singh, S. M. (2011). Maternal voluntary drinking in C57BL/6J mice: Advancing a model for fetal alcohol spectrum disorders. *Behavioural Brain Research*, *223*, 376–387.

Li, H., Xie, Y., Zhang, N., Yu, Y., Zhang, Q., & Ding, S. (2015). Disruption of IP3R2-mediated Ca^{2+} signaling pathway in astrocytes ameliorates neuronal death and brain damage while reducing behavioral deficits after focal ischemic stroke. *Cell Calcium*, *58*, 565–576.

Li, X., Zima, A. V., Sheikh, F., Blatter, L. A., & Chen, J. (2005). Endothelin-1–induced arrhythmogenic Ca^{2+} signaling is abolished in atrial myocytes of inositol-1,4,5-trisphosphate(IP3)–receptor type 2–deficient mice. *Circulation Research*, *96*, 1274–1281.

Mateus-Pinheiro, A., Alves, N. D., Patrício, P., Machado-Santos, A. R., Loureiro-Campos, E., Silva, J. M., … Pinto, L. (2017). AP2γ controls adult hippocampal neurogenesis and modulates cognitive, but not anxiety or depressive-like behavior. *Molecular Psychiatry*, *22*, 1725–1734.

Mederos, S., González-Arias, C., & Perea, G. (2018). Astrocyte–neuron networks: A multilane highway of signaling for homeostatic brain function. *Frontiers in Synaptic Neuroscience*, *10*, 45. https://doi.org/10.3389/fnsyn.2018.00045

Mederos, S., Hernández-Vivanco, A., Ramírez-Franco, J., Martín-Fernández, M., Navarrete, M., Yang, A., … Perea, G. (2019). Melanopsin for precise optogenetic activation of astrocyte-neuron networks. *Glia*, *67*, 915–934.

Mesquita, A. R., Pêgo, J. M., Summavielle, T., Maciel, P., Almeida, O. F. X., & Sousa, N. (2007). Neurodevelopment milestone abnormalities in rats exposed to stress in early life. *Neuroscience*, *147*, 1022–1033.

Navarrete, M., Perea, G., de Sevilla, D. F., Gómez-Gonzalo, M., Núñez, A., Martín, E. D., & Araque, A. (2012). Astrocytes mediate in vivo cholinergic-induced synaptic plasticity. *PLoS Biology*, *10*, e1001259.

Nedergaard, M. (1994). Direct signaling from astrocytes to neurons in cultures of mammalian brain cells. *Science*, *263*, 1768–1771.

Okubo, Y., Kanemaru, K., Suzuki, J., Kobayashi, K., Hirose, K., & Iino, M. (2019). Inositol 1,4,5-trisphosphate receptor type 2-independent Ca^{2+} release from the endoplasmic reticulum in astrocytes. *Glia*, *67*, 113–124.

Oliveira, J. F., Sardinha, V. M., Guerra-Gomes, S., Araque, A., & Sousa, N. (2015). Do stars govern our actions? Astrocyte involvement in rodent behavior. *Trends in Neurosciences*, *38*, 535–549.

Parpura, V., Basarsky, T. A., Liu, F., Jeftinija, K., Jeftinija, S., & Haydon, P. G. (1994). Glutamate-mediated astrocyte-neuron signalling. *Nature*, *369*, 744–747.

Perea, G., Navarrete, M., & Araque, A. (2009). Tripartite synapses: Astrocytes process and control synaptic information. *Trends in Neurosciences*, *32*, 421–431.

Petravicz, J., Boyt, K. M., & McCarthy, K. D. (2014). Astrocyte IP3R2-dependent Ca^{2+} signaling is not a major modulator of neuronal pathways governing behavior. *Frontiers in Behavioral Neuroscience*, *8*, 384.

Petravicz, J., Fiacco, T. A., & McCarthy, K. D. (2008). Loss of IP3 receptor-dependent Ca^{2+} increases in hippocampal astrocytes does not affect baseline CA1 pyramidal neuron synaptic activity. *The Journal of Neuroscience*, *28*, 4967–4973.

Petrelli, F., & Bezzi, P. (2018). mGlu5-mediated signalling in developing astrocyte and the pathogenesis of autism spectrum disorders. *Current Opinion in Neurobiology*, *48*, 139–145.

Pinto-Duarte, A., Roberts, A. J., Ouyang, K., & Sejnowski, T. J. (2019). Impairments in remote memory caused by the lack of Type 2 IP3 receptors. *Glia*, *67*, 1976–1989.

Rakers, C., & Petzold, G. C. (2017). Astrocytic calcium release mediates peri-infarct depolarizations in a rodent stroke model. *Journal of Clinical Investigation*, *127*, 511–516.

Rogers, D. C., Peters, J., Martin, J. E., Ball, S., Nicholson, S. J., Witherden, A. S., … Fisher, E. M. C. (2001). SHIRPA, a protocol for behavioral assessment: Validation for longitudinal study of neurological dysfunction in mice. *Neuroscience Letters*, *306*, 89–92.

Santos, M., Silva-Fernandes, A., Oliveira, P., Sousa, N., & Maciel, P. (2007). Evidence for abnormal early development in a mouse model of Rett syndrome. *Genes, Brain and Behavior*, *6*, 277–286.

Sardinha, V. M., Guerra-Gomes, S., Caetano, I., Tavares, G., Martins, M., Reis, J. S., … Oliveira, J. F. (2017). Astrocytic signaling supports hippocampal–prefrontal theta synchronization and cognitive function. *Glia*, *65*, 1944–1960.

Seibenhener, M. L., & Wooten, M. C. (2015). Use of the open field maze to measure locomotor and anxiety-like behavior in mice. *Journal of Visualized Experiments*, e52434.

Sherwood, M. W., Arizono, M., Hisatsune, C., Bannai, H., Ebisui, E., Sherwood, J. L., … Mikoshiba, K. (2017). Astrocytic IP3Rs: contribution to Ca^{2+} signalling and hippocampal LTP. *Glia*, *65*, 502–513.

Shigetomi, E., Patel, S., & Khakh, B. S. (2016). Probing the complexities of astrocyte calcium signaling. *Trends in Cell Biology*, *26*, 300–312.

Silva-Fernandes, A., Duarte-Silva, S., Neves-Carvalho, A., Amorim, M., Soares-Cunha, C., Oliveira, P., … Maciel, P. (2014). Chronic treatment with 17-DMAG improves balance and coordination in a new mouse model of Machado-Joseph disease. *Neurotherapeutics*, *11*, 433–449.

Sousa, N., Almeida, O. F. X., & Wotjak, C. T. (2006). A hitchhiker's guide to behavioral analysis in laboratory rodents. *Genes, Brain and Behavior*, *5*, 5–24.

14609568, 2021, 5, Downloaded from https://onlinelibrary.wiley.com/doi/10.1111/ejn.14724 by Universidade Do Minho, Wiley Online Library on [16/10/2026]. See the Terms and Conditions (https://onlinelibrary.wiley.com/terms-and-conditions) on Wiley Online Library for rules of use; OA articles are governed by the applicable Creative Commons License

Srinivasan, R., Huang, B. S., Venugopal, S., Johnston, A. D., Chai, H., Zeng, H., … Khakh, B. S. (2015). Ca^{2+} signaling in astrocytes from Ip3r2-/- mice in brain slices and during startle responses in vivo. *Nature Neuroscience*, *18*, 708–717.

Takata, N., Mishima, T., Hisatsune, C., Nagai, T., Ebisui, E., Mikoshiba, K., & Hirase, H. (2011). Astrocyte calcium signaling transforms cholinergic modulation to cortical plasticity in vivo. *Journal of Neuroscience*, *31*, 18155–18165.

Tanaka, M., Shih, P.-Y., Gomi, H., Yoshida, T., Nakai, J., Ando, R., … Itohara, S. (2013). Astrocytic Ca^{2+} signals are required for the functional integrity of tripartite synapses. *Molecular Brain*, *6*, 6.

Tanaka, M., Wang, X., Mikoshiba, K., Hirase, H., & Shinohara, Y. (2017). Rearing-environment-dependent hippocampal local field potential differences in wild-type and inositol trisphosphate receptor type 2 knockout mice. *Journal of Physiology*, *595*, 6557–6568.

Tavares, G., Martins, M., Correia, J. S., Sardinha, V. M., Guerra-Gomes, S., das Neves, S. P., … Oliveira, J. F. (2017). Employing an open-source tool to assess astrocyte tridimensional structure. *Brain Structure and Function*, *222*, 1989–1999.

Teixeira-Castro, A., Jalles, A., Esteves, S., Kang, S., da Silva Santos, L., Silva-Fernandes, A., … Maciel, P. (2015). Serotonergic signalling suppresses ataxin 3 aggregation and neurotoxicity in animal models of Machado-Joseph disease. *Brain*, *138*, 3221–3237.

Verkhratsky, A., & Nedergaard, M. (2016). The homeostatic astroglia emerges from evolutionary specialization of neural cells. *Philosophical Transactions of the Royal Society B: Biological Sciences*, *371*, 20150428.

Volterra, A., Liaudet, N., & Savtchouk, I. (2014). Astrocyte Ca^{2+} signalling: An unexpected complexity. *Nature Reviews Neuroscience*, *15*, 327–335.

Wang, F., Xu, Q., Wang, W., Takano, T., & Nedergaard, M. (2012). Bergmann glia modulate cerebellar Purkinje cell bistability via Ca^{2+}-dependent K^{+} uptake. *Proceedings of the National Academy of Sciences*, *109*, 7911–7916.

Yang, J., Yang, H., Liu, Y., Li, X., Qin, L., Lou, H., … Wang, H. (2016). Astrocytes contribute to synapse elimination via type 2 inositol 1,4,5-trisphosphate receptor-dependent release of ATP. *eLife*, *5*, e15043.

Yu, X., Nagai, J., & Khakh, B. S. (2020). Improved tools to study astrocytes. *Nature Reviews Neuroscience*, *21*(3), 121–138.

Yu, X., Taylor, A. M. W., Nagai, J., Golshani, P., Evans, C. J., Coppola, G., & Khakh, B. S. (2018). Reducing astrocyte calcium signaling in vivo alters striatal microcircuits and causes repetitive behavior. *Neuron*, *99*, 1170–1187.e9.

How to cite this article: Guerra-Gomes S., Cunha-Garcia D., Marques Nascimento D. S., et al. (2021). IP_3R2 null mice display a normal acquisition of somatic and neurological development milestones. *European Journal of Neuroscience, 54*(5), 5673–5686. https://doi.org/10.1111/ejn.14724

14609568, 2021, 5, Downloaded from https://onlinelibrary.wiley.com/doi/10.1111/ejn.14724 by Universidade Do Minho, Wiley Online Library on [16/10/2026]. See the Terms and Conditions (https://onlinelibrary.wiley.com/terms-and-conditions) on Wiley Online Library for rules of use; OA articles are governed by the applicable Creative Commons License